Omnifocus image synthesis using Lens Swivel

Create an all-in-focus image by fusing multiple images taken under lens rotations? It's all about the pupils!

Indranil Sinharoy — isinharoy@smu.edu
Prasanna Rangarajan — prangara@smu.edu
Marc P. Christensen — mpc@lyle.smu.edu

Introduction

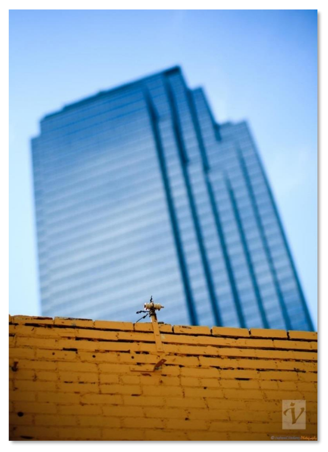

An omnifocus image has everything in the close foreground to far background in sharp focus.

Lenses can focus only on a single surface—usually, the *plane* of sharp focus—as dictated by the laws of physics. Consequently, objects fore and aft the plane of sharp focus gradually get out of focus and appear blurry in the image. This interplay of light and lenses leads to the limited depth of field (DOF) problem.

Several methods overcome this problem. For example, wavefront coding, plenoptic imaging, Scheimpflug imaging, focus stacking, etc.

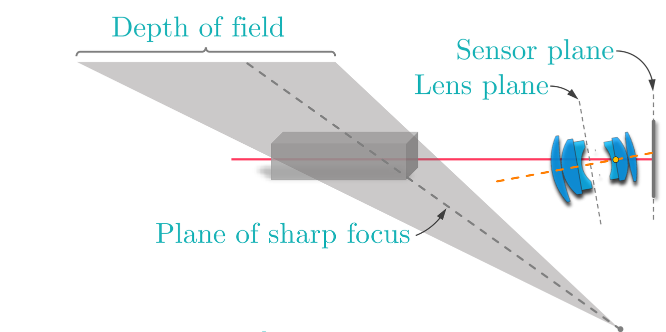

In Scheimpflug imaging the lens or the sensor or both are rotated, which induces a rotation of the plane of sharp focus allowing scenes with significant depths to be in focus.

In focus stacking, images are captured at multiple focus depths. Therefore, regions only at specific depths are in focus in a single image. Collectively, however, the stack contains the whole scene in focus distributed amongst the images.

An omnifocus image is created by registering the images, followed by identifying and blending the in-focus regions.

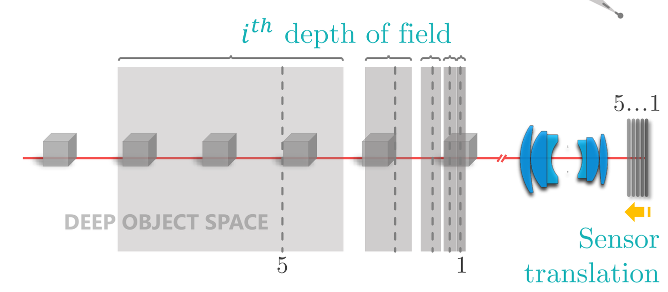

The DOF region in Scheimpflug imaging is still limited. Significant portions of each DOF region in focus stacking extends beyond the field-of-view of the imager resulting in suboptimal utilization. We present a method for creating omnifocus images, building on the essential elements from Scheimpflug imaging and focus stacking, which consists of compositing from a stack of images obtained under multiple lens rotations.

Geometric model

Relation between object point $\mathbf{x}$ and image point $\acute{\mathbf{x}}$:

$$ {}^{I}\acute{\mathbf{x}} = R_i^T\left(\acute{d}_e\, \mathbf{r}_{\ell,3} - \mathbf{t}_i\right) + \frac{\left(\hat{\mathbf{n}}_i(3)\acute{z}_o - \acute{d}_e \hat{\mathbf{n}}_i^T \mathbf{r}_{\ell,3}\right)}{\hat{\mathbf{n}}_i^T R_\ell M_p R_\ell^T\left({}^{C}\mathbf{x} - d_e\, \mathbf{r}_{\ell,3}\right)} R_i^T R_\ell M_p R_\ell^T\left({}^{C}\mathbf{x} - d_e\, \mathbf{r}_{\ell,3}\right) \quad (1)$$

where, $M_p = \begin{bmatrix} 1 & 0 & 0 \\ 0 & 1 & 0 \\ 0 & 0 & m_p \end{bmatrix}$, $\mathbf{t}_i = [0, 0, \acute{z}_o]^T$.

The entrance and exit pupils are the images of the limiting aperture. The entrance pupil is the center of projection on the object side.

The pupil magnification, $m_p = \frac{\acute{h}_e}{h_e} = \frac{\tan(\omega)}{\tan(\acute{\omega})}$. (2)

The corresponding points between two images obtained under different lens rotations are related by a transformation called the inter-image homography.

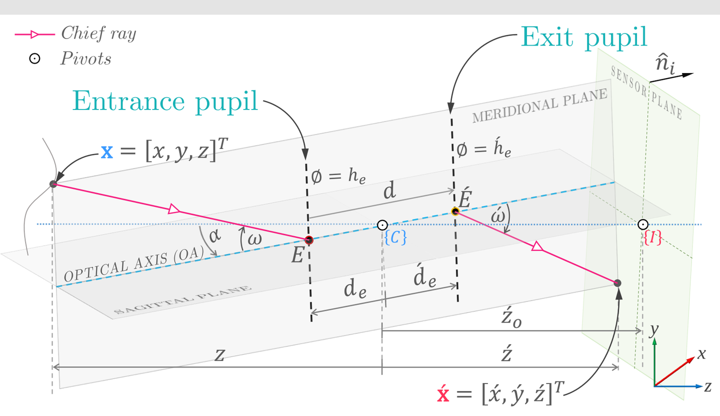

$\{C\}, \{I\}$: Camera and Image coordinate frames. Origin of $\{C\}$ is coincident of the pivot.
$E, \acute{E}$: Center of entrance & exit pupils resp.
$d_e, \acute{d}_e$: Loc. of ent. & exit pupils resp. from the pivot.
R_ℓ: Rotation matrix; orientation of lens plane.
$\mathbf{r}_{\ell,3}$: 3rd column of R_ℓ (optical axis).
R_i: Rotation matrix; orientation of sensor plane.
$\hat{\mathbf{n}}_i$: Normal to sensor plane.
$\acute{z}_o$: Distance of image plane from pivot.

Inter-image homography for lens tilt about the entrance pupil, if $\acute{x}_n$ & $\acute{x}_m$ are corresponding points:

$$\acute{x}_n = \left[\mathbf{p}\, \mathbf{s}\, R_{\ell;n} M_p R_{\ell;n}^T\, R_{\ell;m} M_p^{-1} R_{\ell;m}^T + \frac{d}{\hat{\mathbf{n}}_i(3)\,\acute{z}_o}\left(\mathbf{r}_{\ell,3;n} - \mathbf{p}\,\mathbf{s}\, R_{\ell;n} M_p R_{\ell;n}^T\, R_{\ell;m} M_p^{-1} R_{\ell;m}^T\right)\hat{\mathbf{n}}_i^T \right] \acute{x}_m \quad (3)$$

where, $\mathbf{p} = \frac{(\hat{\mathbf{n}}_i(3)\acute{z}_o - d\, \hat{\mathbf{n}}_i^T \mathbf{r}_{\ell,3;n})}{(\hat{\mathbf{n}}_i(3)\acute{z}_o - d\, \hat{\mathbf{n}}_i^T \mathbf{r}_{\ell,3;m})}$, $\mathbf{s} = \frac{(\hat{\mathbf{n}}_i^T R_{\ell;m} M_p R_{\ell;m}^T \mathbf{x})}{(\hat{\mathbf{n}}_i^T R_{\ell;n} M_p R_{\ell;n}^T \mathbf{x})}$

If **pupil magnification = 1**, the inter-image homography between the reference image (for no lens tilt) and an image obtained under a lens rotation of α, reduces to a simple scaling & translation transformation:

$$\acute{x}_n = \underbrace{\begin{bmatrix} (d\cos\alpha - \acute{z}_o)/(d - \acute{z}_o) & 0 & 0 \\ 0 & (d\cos\alpha - \acute{z}_o)/(d - \acute{z}_o) & d\sin\alpha \\ 0 & 0 & 1 \end{bmatrix}}_{\text{Inter-image homography, } H} \acute{x}_0 \quad (4)$$

Further, to focus on an object plane at a distance z_o (measured from the entrance pupil) and tilted by an angle β about the x-axis by rotating the lens (about its entrance pupil), the following conditions must be satisfied:

Image plane distance:

$$\acute{z}_o = d\cos\alpha + \frac{m_p z_o f(m_p \cos^2\alpha + \sin^2\alpha)}{m_p z_o \cos\alpha + f} \quad (5)$$

The object plane tilt β is related to the lens plane tilt angle α as:

$$\tan\beta = -\frac{\sin\alpha\,[m_p z_o + f(1 - m_p)\cos\alpha]}{f(m_p\cos^2\alpha + \sin^2\alpha)} \quad (6)$$

Substituting $x = \cos\alpha$ and $y = \sin\alpha$ in Eq. 6:

$$f m_p \tan\beta\, x^2 + f\tan\beta\, y^2 + f(1 - m_p)xy + m_p z_o y = 0 \quad (7)$$

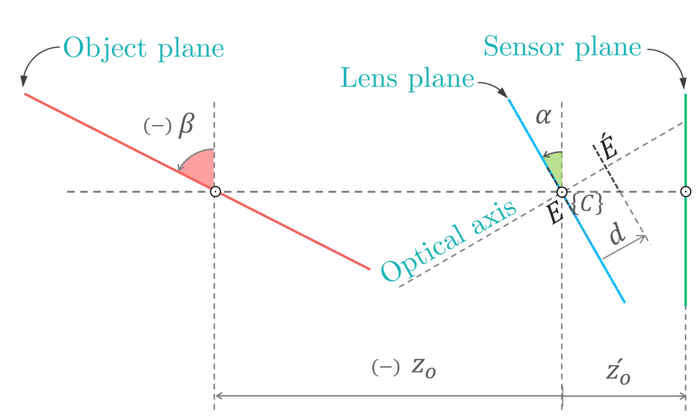

The above quadratic curve expression can be used to determine α for known values of β.

Simulation in Zemax with PyZDDE

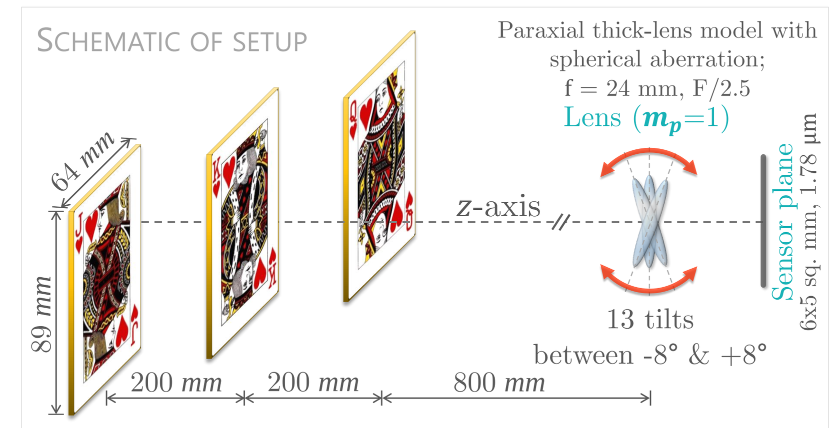

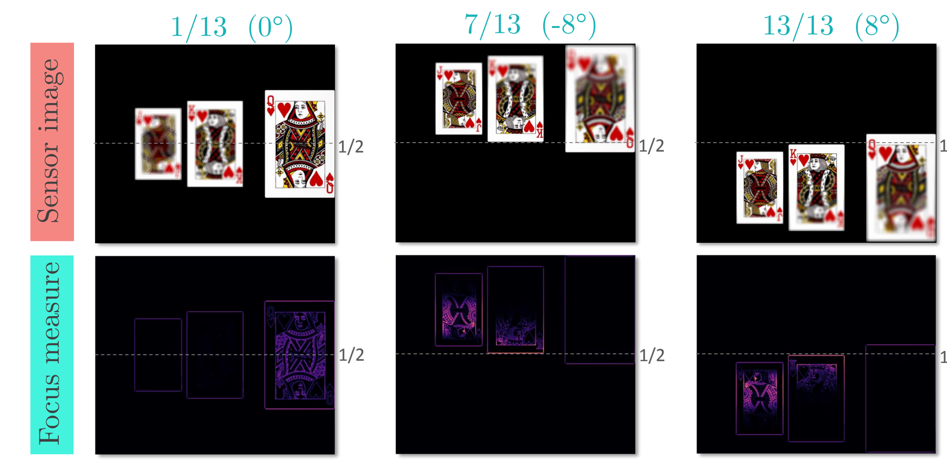

The top left figure shows the setup of a simulation in Zemax in which a 24 *mm*, F/2.5 symmetric lens (m_p=1) was used to image three playing cards for 13 lens rotations of the lens about the entrance pupil. We have shown 3 (out of 13) images of the scene as it appears on the sensor above. Notice the transverse shift in the image field between the images as predicted by Eq. 4. The in-focus regions of the scene, detected using a Laplacian of Gaussian filter, are also shown above. Notice when the lens is tilted, portions of all three cards in focus.

Following precise registration of the images in the stack using the inter-image homography H, we selectively blend the portions of the scene that are in focus to create a composite image in which all three cards appear sharp.

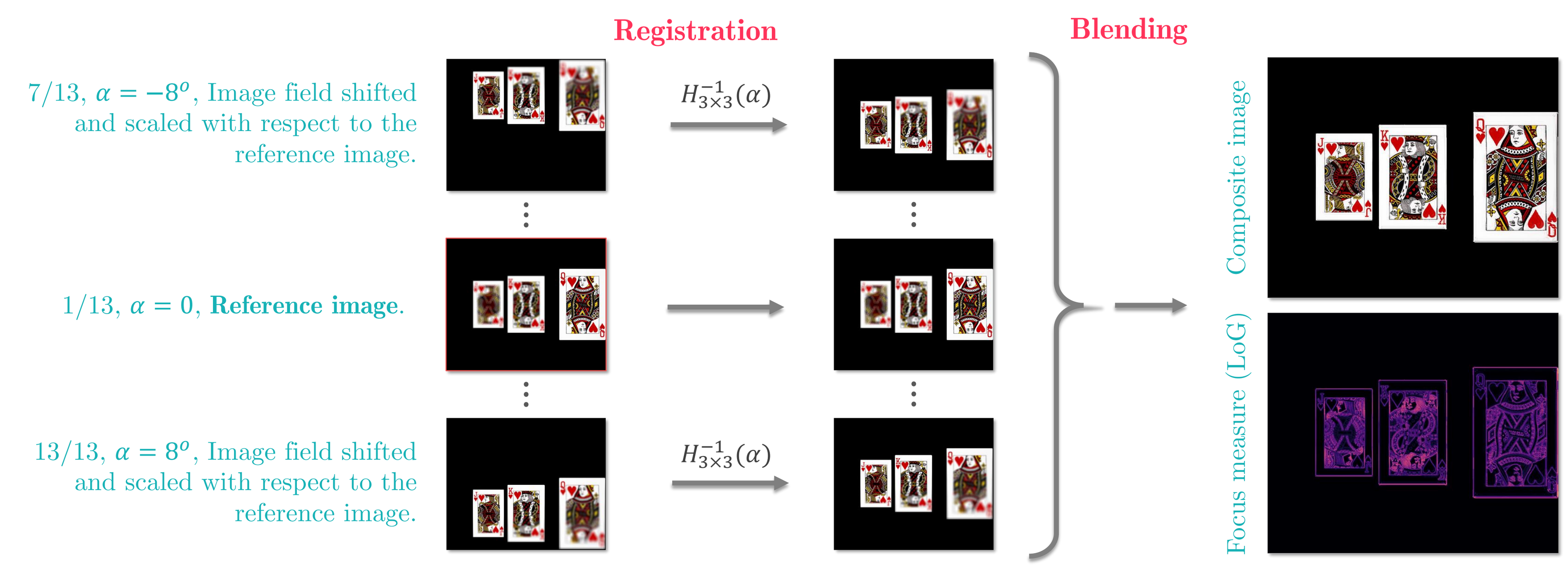

Discussion

Advantages and comparison with frontoparallel focus stacking

- The registration using closed form equation is simple, esp. if the pupil magnification of the lens is one.
- Can be used to improve the depth of field around a tilted object plane in Scheimpflug imaging.

What if the pupil magnification of the lens is different from one?

The rotation of the lens induces a shift and scaling of the image field. If the pupil magnification is one, the scaling is uniform and the shift is simple. If the pupil magnification is different from one, then anisotropic shift across the image field manifests as image distortion.

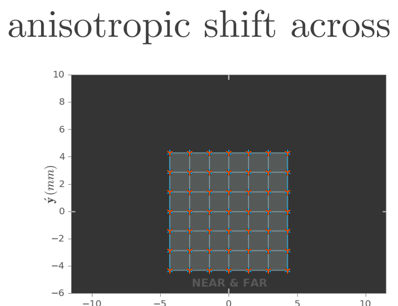

Coincident grid of image points from two planes at different depths.

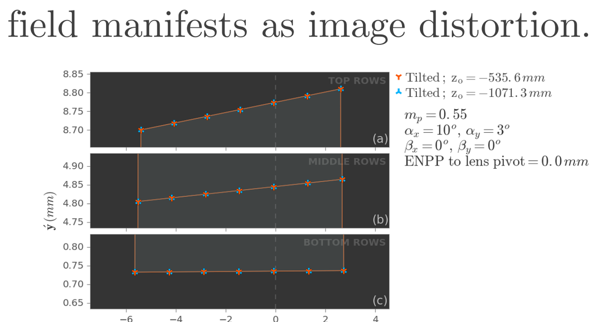

The top, middle and bottom rows of the grid, following lens rotation. $m_p = 0.55$

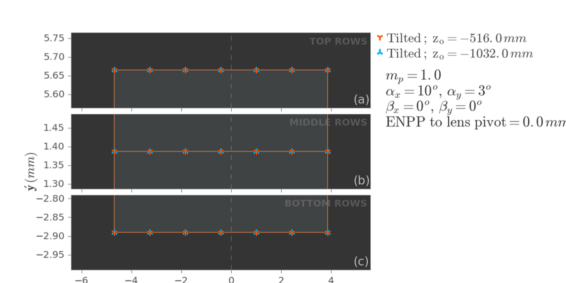

The top, middle and bottom rows of the grid, following lens rotation. $m_p = 1.0$

What if we rotate the lens about a point away from the entrance pupil?

If the lens is rotated about a point away from the entrance pupil then amount of shift experienced by points in the image field is dependent on depth (parallax). Then, registering becomes hard.

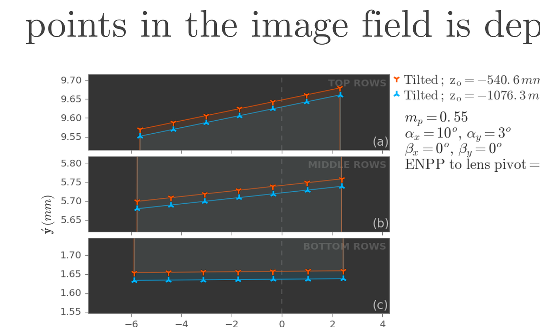

The top, middle and bottom rows of the grid, following lens rotation about a point away from the entrance pupil. $m_p = 0.55$

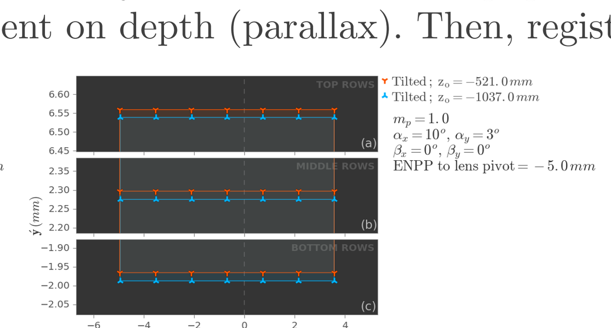

The top, middle and bottom rows of the grid, following lens rotation about a point away from the entrance pupil. $m_p = 1.0$

What if need to increase the depth of field just around a tilted object surface of known tilt angle β?

First we need to determine the required lens rotation angle α. While Eq. 6 yields β in terms of α, obtaining an inverse relationship for α given β is hard. Instead, we use Eq. 7 which yields a quadratic curve for the given parameters. The lens tilt α is then obtained as the intersection of the quadratic curve and the unit circle as shown to the right.

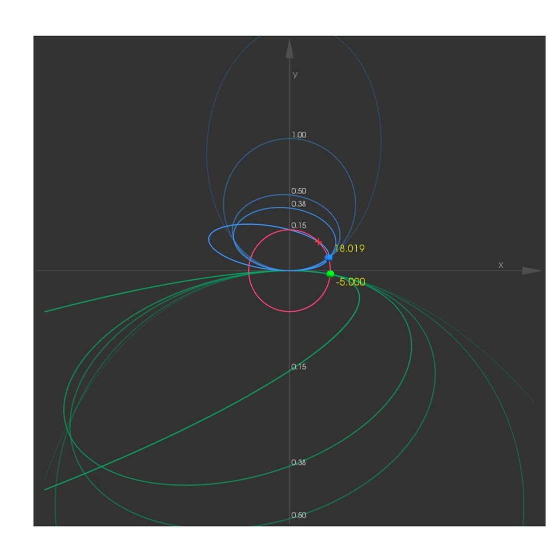

SMU.
Photonics Architecture Lab, Lyle School of Engineering,
Southern Methodist University, Dallas, Texas, USA.

References

[1] C. H. Anderson, J. R. Bergen, P. J. Burt, J. M. Ogden, "Pyramid Methods in Image Processing," RCA Engineer, vol. 29, pp. 33-41 (1984).

[2] Jacobson, Ralph, Sidney Ray, Geoffrey G. Attridge, and Norman Axford, *Manual of Photography* (Taylor & Francis, 2000), Chap. 10.

[3] Indranil Sinharoy, Prasanna Rangarajan, and Marc P. Christensen, "Geometric model of image formation in Scheimpflug cameras," PeerJ Preprints 4:e1887v1 https://doi.org/10.7287/peerj.preprints.1887v1 (2016).

[4] Indranil Sinharoy *et al.*, PyZDDE: Release version 2.0.2. Zenodo. 10.5281/zenodo.44295 (2016).

[5] Open source tools: PyZDDE NumPy matplotlib jupyter h5py

indranilsinharoy.com/projects/omnifocus